DVS SLV HALLE

YPIC 2017

3RD YOUNG WELDING PROFESSIONALS INTERNATIONAL CONFERENCE

August 16th – 18th, 2017
Halle (Saale), Germany
CONFERENCE BOOK

Table of contents

Main sponsor

DVS Welding Society, Düsseldorf, Germany

Gold sponsors

EWM AG, Mündersbach, Germany

Kemppi GmbH, Lahti, Finland

TÜV Nord Systems GmbH & Co. KG, Hamburg, Germany

Kjellberg Finsterwalde Plasma und Maschinen GmbH, Finsterwalde, Germany

Gas tungsten arc welding of different high strength austenitic stainless steel grades

Ing. student Eszter Kalácska, Dr.-Ing Kornél Májlinger, Dipl.-Ing. Balázs Varbai, Budapest, Hungary

1 Introduction

Stainless steels contain more than 10.5 % chromium and less than 1.2 % carbon as an alloying element. According to the microstructure and their usability, stainless steels could be separated to five different, corrosion resistant types, such as: austenitic, ferritic, martensitic, duplex (austenitic – ferritic) and precipitation hardened. Among all of these, the austenitic types play the main role in industrial applications. Recently, the usage of austenitic steels is increased to 75 % among all the stainless steel types [1]. According to the alloying elements, austenitic stainless steels could be separated to chromium-nickel (Cr-Ni) and chromium-manganese (Cr-Mn) types. The Cr-Ni steels usually contain 16 to 19 % Cr and 6 to 12 % Ni (the most popular types are 1.4301 (AISI 304) and 1.4430 (AISI 316). Because of the recent fluctuations of Ni price [2], stainless steel producer companies made efforts in order to decrease the Ni content in these steels. Manufacturers payed emphasized attention in using Mn (5–11 %) and N (< 0.25 %) as alloying elements [2–11]. These steels marked as AISI 200 series. The usage of the Cr-Mn alloyed austenitic steels are constantly growing, especially in Asia [12]. According to steel manufacturers predictions the usability of Cr-Mn steels will reach 20 % by the end of 2010's (from 9 % in the beginning of the 21st century) among all of the stainless steels [1, 2, 4, 7]. Beside their low cost (currently nickel is around five times more expensive than manganese on metal stock market [13]), the N (> 0.13 %) alloyed austenitic steels have higher yield strength (~ 400 MPa), than the conventional Cr-Ni steels (~ 300 MPa), which is also a highlighted research area [5, 6, 8, 10, 14, 15]. Researchers [6] showed that with increasing nitrogen content in solid solution, the yield and tensile strengths also higher. Increasing the dissolved N content from 0 to 0.2 % the yield strength doubles from 200 to 400 MPa in these steels. The increasing mechanical strength makes the manganese alloyed austenitic steels possible for structural applications [16]. Beside the lower cost and better mechanical properties of Cr-Mn steel, their corrosion resistance is usually lower, than the Cr-Ni types [17, 18]. The reason for this is the relatively high Mn and low Ni content, but the high (> 0.1 %) N content improves the pitting corrosion resistance [19] and the Cr-Mn alloyed austenitic steel have better performance in terms of transgranular stress corrosion [20]. The recently developed pitting resistance equivalent numbers (such as PRE_{Mn}, MARC, IRCL) all calculates with the negative effect of Mn [11, 21]. From weldability standpoint the Cr-Mn steels behave generally the same as Cr-Ni steels. In case of higher N addition to the base metal (BM) and fast welding travel speed porosity formation was experienced in some cases [20, 22]. The decreasing N content in the weld metal (WM) (due to porosity formation) resulting in increasing ferrite number. As conventional austenitic grades, the ones with higher carbon content are also sensible for $M_{23}C_6$ carbide formation (sensitization). The formation of these carbides reducing stress corrosion cracking resistance [23] and the volume of carbides is increasing with increasing number of welding passes [24]. Reducing nickel content also increasing the sensitization tendency, as Ni lowers the carbon solubility in austenite [18]. Also, because of the increased N and Cr content, researchers [25] found Cr_2N precipitation after 1 hour ageing at 850°C temperature in Mn (19 %) and N (0.5 %) over alloyed austenitic grade. All the nitrogen containing steels primarily solidify as delta ferrite, which helps the resistance against hot cracking [19]. The autogeneous welding of Cr-Mn steels are not well published [24]. Comparing to the conventional grades, during gas tungsten arc welding (GTAW or TIG) the Cr-Mn steels behaves generally the same as the CrNi grades, apart from some special behaviours [26, 27]. Researchers [28] investigated the effects of welding speed during TIG welding of 1.4372 (AISI 201) material. As the welding speed increases, the heat input decreased, which refers in narrower weld pool width and decreasing grain coarsening. The higher welding speed also means smaller dendrite size and higher tensile strength and ductility and the corrosion properties improved. The best mechanical and corrosion properties were measured with high, 3.5 $mm \cdot s^{-1}$, welding speed. Using active flux coating on the surface [29] resulting in the same improvement of the welding process as in case of activated flux welding (A-TIG) of other stainless steels [30]. The weldability with other resistance and fusion welding processes is not well published, but researchers made experiments in shielded metal arc welding [26, 31, 32], laser beam welding [33], plasma arc welding [34] and resistance spot welding [35].

Therefore, in our research we investigated the weldments of four steel grades; one commercial Cr-Ni austenitic steel grade, and three high strength grades with increased nitrogen content, of which two grades were Cr-Mn-N alloyed.

2 Materials and methods

For the welding tests three grades of high strength and as comparison one normal strength austenitic stainless steels were used. The base materials were the following grades: 1.4371, 1.4376, 1.4318 and 1.4301 with sheet thicknesses of: 2.28, 1.92, 2 and 2 mm respectively. As welding method, manual GTAW was used, with two types of filler rods: 1.4316 (308 L Si) and 1.4430 (316 L Si) in 2.4 mm diameters. The chemical composition of the used materials are listed in Tab.1, the nominal values were also controlled by a PMI Master Sort emission spectrometer.

Table 1. *Chemical composition of the used steel sheets and filler metals*

Steel grade	Chemical composition (wt%)								
	C	Cr	Ni	Mn	Si	Mo	Cu	N	Fe
1.4371	0.05	15.8	*4.4*	*7.7*	0.5	0.1	0.4	*0.2*	bal.
1.4376	0.11	17.1	*3.8*	*7.2*	0.6	-	0.5	*0.2*	bal.
1.4318	0.05	16.5	7.3	1.6	0.5	0.2	0.3	*0.2*	bal.
1.4301	0.05	18.3	8.6	1.8	0.4	0.2	0.4	-	bal.
1.4316	0.02	19.0	9.5	1.8	0.9	-	-	-	bal.
1.4430	0.02	18.5	12.5	1.8	0.9	2.6	-	-	bal.

The samples for quantitative metallography and micro hardness testing was mounted in metallography resin, mechanically grounded with SiC papers from P80 to P4000 beside continuous water rinse, polished (with 1 µm and 0.5 µm grain size Al_2O_3 emulsion) and finally chemically etched. As etchant methanolic aqua regia (45 ml HCl + 15 ml HNO_3 + 20 ml methanol) and Kalling reagent (2 g $CuCl_2$ + 40 ml HCl + 40 ml C_2H_6O) were used. The methanolic aqua regia etchant applied for 20 s proved to be more effective than the Kalling reagent in order to reveal the grain structure. Optical microscopy with Olympus PM3 microscope was performed on etched specimens for the determination of grain structures. The grain structure of the four steel sheets can be seen in Fig.1. The main properties of the used materials are listed in Tab. 2.

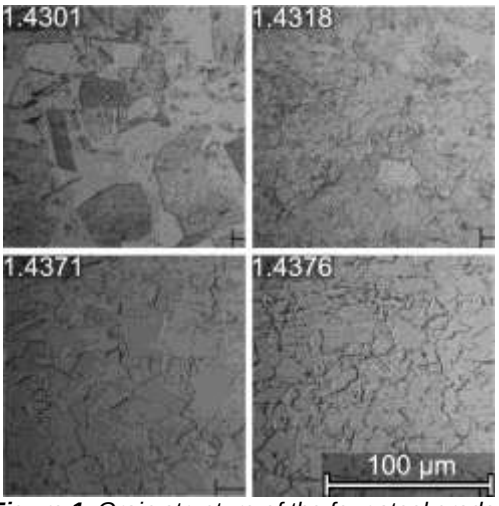

Figure 1. *Grain structure of the four steel grades*

Also, microhardness measurements on the joints were made with Buehler 1011 type microhardness tester, to evaluate hardness changes throughout the weldments. The micro Vickers hardness tests were made on the metallographic, etched specimens. Hardness measurements were made perpendicularly to the welding line, across the fusion zone in the WM and heat effected zone (HAZ) HAZ 1 denotes the zone close to the molten WM and HAZ 2 further away. Vickers indentations were performed using a step size of 0.3 mm and a 500 g load (HV0.5), according the ASTM E384 standard.

Table 2. *Main properties of the used materials*

Steel grade	Main properties				
	$R_{p0.2}$ (MPa)	R_m (MPa)	$A_{11.3}$ (%)	Hardness (HV0.5)	Grain size (µm)
1.4371	620	760	25	277±10	12
1.4376	405	740	40	251±10	11
1.4318	350	660	35	205±2	10
1.4301	190	620	35	187±5	22
1.4316	390	590	35	195±4	-
1.4430	430	650	34	200±4	-

For the welding tests 130×60 mm sheets were cut out, without edge chamfering. The sheets were cleaned before the tests with acetone. Butt welded joints were produced with ESAB Aristotig 250 welding machine using two different filler materials, perpendicularly to the roll direction to obtain 130×120 mm specimens. The sheets were mechanically clamped before welding; they were not in direct contact to each other, at the end of the sheets ~1 mm gap existed to provide co-axial joints. The thickness step (max. 0.26 mm) of the sheets was on the face side of the joint.

To protect the weld bead from environmental contaminantion and oxidation pure argon 4.6 (99.996 % Ar) shielding gas was used during welding on the face and root side, with a flow rate of 10 and 8 $l \cdot min^{-1}$ respectively. The welded specimens were also mechanically clamped during their cooling procedure, they were fastened in the clamping device until the temperature in the joint and heat affected zone reached the 50^0C temperature.

The welding parameters; current (I), voltage (U), welding speed (v), heat input (Q) and the different materials combinations for the joints are listed in Tab 3. As you can see the heat input was kept low, between 0.27 – 0.39 $kJ \cdot mm^{-1}$.

Table 3. *Welding parameters and joint combinations for the different filler materials for manual GTAW*

	Sheet grade	Sheet grade	Welding parameters			
			I (A)	U (V)	v ($cm \cdot min^{-1}$)	Q ($kJ \cdot mm^{-1}$)
1.4316 filler	**1.4371**	**1.4371**	75	11.7	10.7	0.30
	1.4371	**1.4376**	75	11.5	11.6	0.27
	1.4371	**1.4318**	75	11.5	8.0	0.39
	1.4371	**1.4301**	75	11.7	8.4	0.38
	1.4376	**1.4376**	75	11.3	10.5	0.29
	1.4376	**1.4318**	75	11.5	10.0	0.31
	1.4376	**1.4301**	75	11.5	9.3	0.33
1.4430 filler	**1.4371**	**1.4371**	75	11.7	9.0	0.35
	1.4371	**1.4376**	75	11.3	9.2	0.33
	1.4371	**1.4318**	75	11.2	10.5	0.29
	1.4371	**1.4301**	75	11.3	9.6	0.32
	1.4376	**1.4376**	75	11.7	9.2	0.34
	1.4376	**1.4318**	75	11.3	10.4	0.29
	1.4376	**1.4301**	75	11.2	10.3	0.29

For the determination of the tensile characeristics of the welded joints quasistatic tensile tests were carried out with MTS 810 universal materials testing machine. The tensile specimens were cut out in a way that their longitudinal axis was perpendicular to the welding line. Tensile tests were performed under quasi-static loading condition, using a constant crosshead speed of 3 $mm \cdot min^{-1}$, according to EN ISO 6892-1 standard. Tensile tests were carried out on every combinations and three welded samples were investigated for each welded joint, to receive consistent results.

3 Results and discussion

The face and root sides of the welded joints can be seen in Fig. 3–4 for the two filler metals. It is clear, that the welding parameters in Tab. 3 are appropriate to produce discontinuity free joints with even face and root sides. Therefore, the joints welded with the listed parameters were examined more in details.

Microstructure and grain coarsening

All the weldments were austenitic of course; in the sheets with polygonal grains and in the weldment with dendritic structure (Fig.5). To compare the grain coarsening of the different material grades, grain sizes were determined on metallographic images e.g. Fig.5. The grain sizes measured in the different heat affected zones of the joints are listed in Tab. 4. To compare the different austenitic steel grades these gran sizes were normalized to their own base material grain sizes of Tab.2 and visualized in Fig.5.

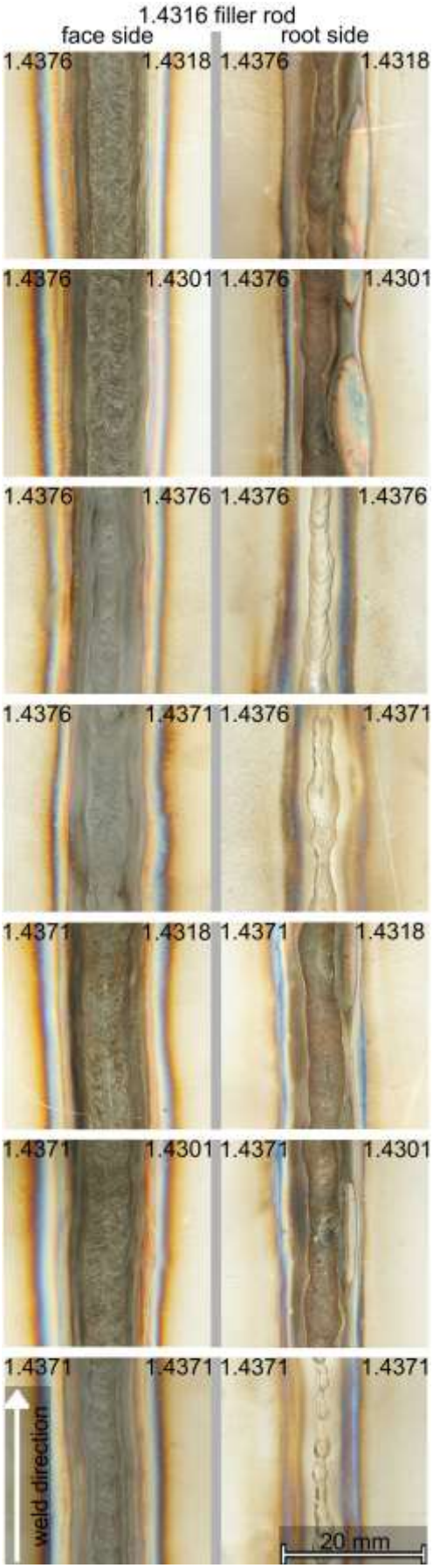

Figure 3. *Macroimages from the face side (left) and root side (right) of the different joints welded with 1.4316 filler material*

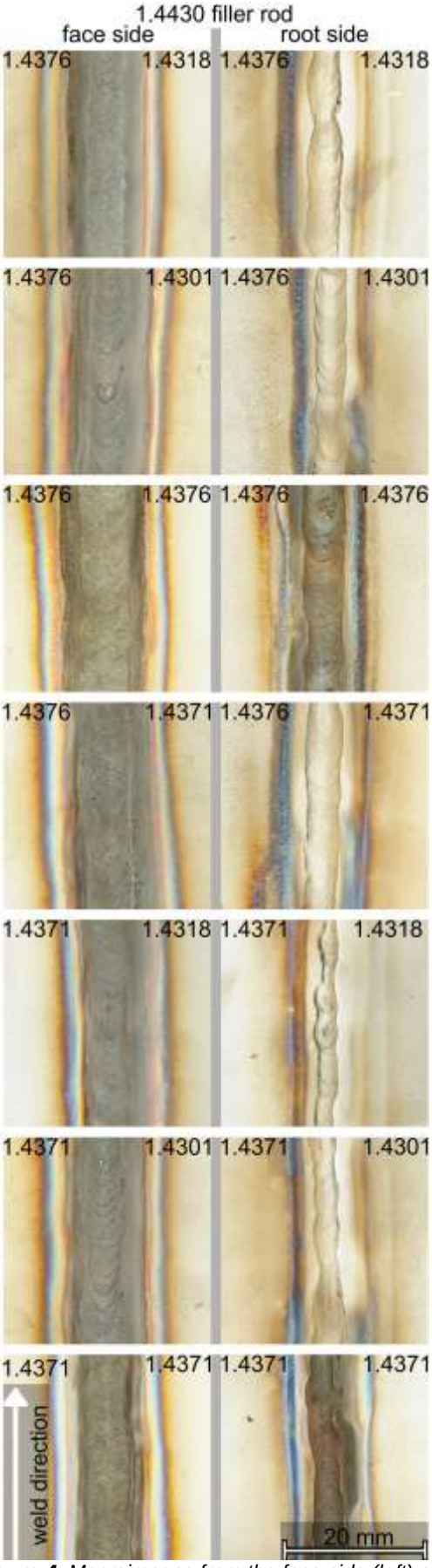

Figure 4. *Macroimages from the face side (left) and root side (right) of the different joints welded with 1.4430 filler material*

Table 4. *Measured grain sizes in the different joints in the HAZ, according to ASTM E112*

	Sheet grade	Grain sizes (µm) HAZ2	HAZ1	HAZ1	HAZ2	Sheet grade
1.4316 filler	**1.4371**	9	37	34	14	**1.4371**
	1.4371	13	34	26	11	**1.4376**
	1.4371	13	44	35	15	**1.4318**
	1.4371	15	44	50	18	**1.4301**
	1.4376	12	25	29	11	**1.4376**
	1.4376	11	27	35	14	**1.4318**
	1.4376	11	23	38	14	**1.4301**
1.4430 filler	**1.4371**	15	40	37	17	**1.4371**
	1.4371	14	40	27	12	**1.4376**
	1.4371	15	37	29	17	**1.4318**
	1.4371	15	35	42	16	**1.4301**
	1.4376	12	29	29	11	**1.4376**
	1.4376	11	22	29	13	**1.4318**
	1.4376	11	22	32	13	**1.4301**

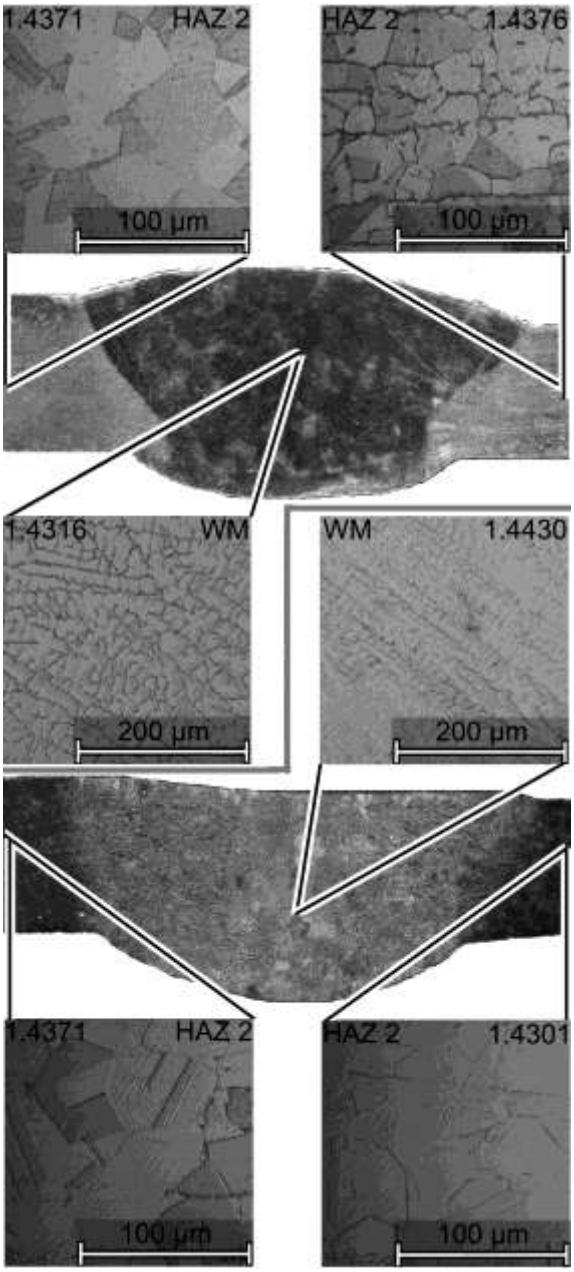

Figure 5. *Macroimages from two joints welded with different filler metals, and enlarged microscope images from the HAZ 2 and WM*

According to Tab 4 the average grain sizes were under 50 µm in all cases. However, in some cases the grain coarsening in the HAZ zones was very different for the different grades (Fig.5).

In the HAZ 1 of the 1.4371 Cr-Mn austenitic grade and the 1.4318 Cr-Ni austenitic grade had approx. the same grain coarsening, smaller grain coarsening was observed in the 1.4376 and 1.4301.

In the HAZ 2 region had the 1.4318 steel grade the largest grain coarsening effect, smaller had the 1.4371 grade, and the 1.4376 (other Cr-Mn alloying) had almost the initial grain size and no coarsening compared to the initial state. The 1.4301 grade had the lowest grain coarsening compared to the other grades both in HAZ 1 and in HAZ 2. In HAZ 2, presumably due to the fast cooling rate (and larger grains of the BM) the grain size was even a bit smaller than before welding.

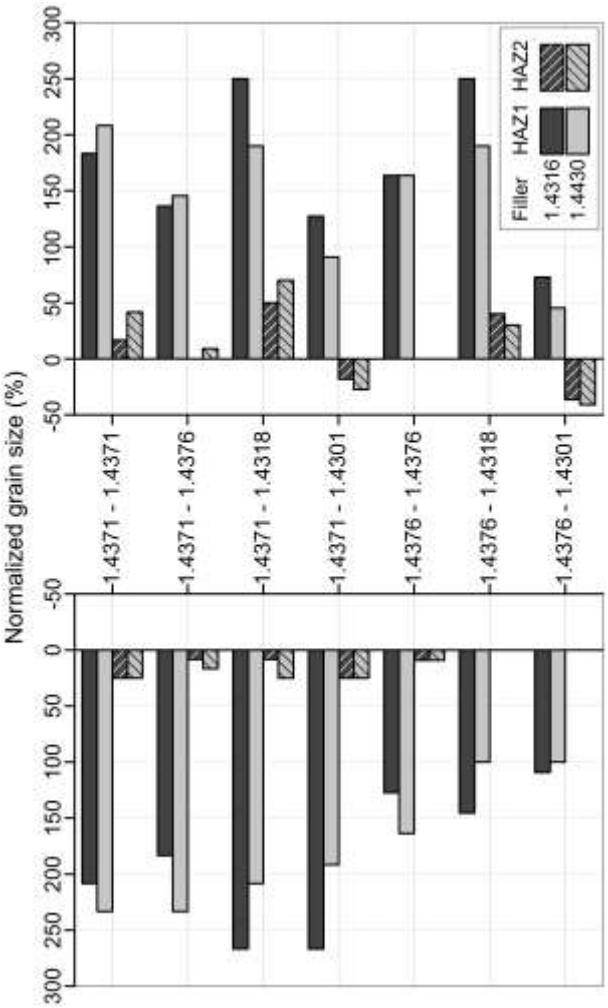

Figure 5. *To the initial grain size nomalized grain sizes of in the HAZ-s of the different joint types*

Tensile properties

The ultimate tensile strength (R_m) of the base materials were all higher than the filler materials (Tab. 2.), therefore the fracture always occurred within the weld material (e.g. Fig. 6).

As we can see in in Fig. 7 the ultimate tensile strength values were all over 600 MPa. The lowest strength had the joints with the 1.4301 material (which has also the lowest R_m). The highest strength were measured on the joints containing 1.4371 and/or 1.4376 steels – which had also the highest R_m – and possibly because of the dilution with the filler metal also the R_m increased above the tensile strength values of the 1.4316 weld metal. In case of the 1.4430 filler the 1.4371-1.4318 and the 1.4376-1.4318 joint had R_m over the tensile strength of the filler metal.

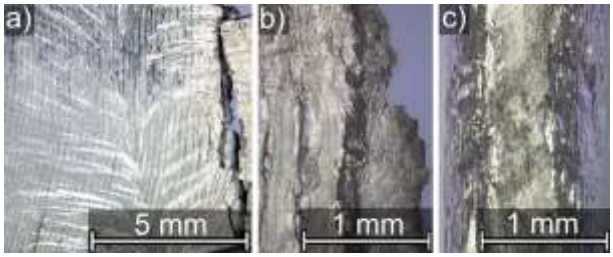

Figure 6. *Stereomicroscope images of the fractured tensile specimen (1.4376-1.4376 joint with 1.4430 filler); a),b) deformed weld metal surface and c) the fracture surface*

As for the fracture elongations ($A_{11.3}$) every joint was above 12% but only two of them reached the (1.4376-1.4318 and 1.4376-1.4301) 25 % (the nominal fracture elongation value for the least deformable 1.4371 grade) (Fig. 8). Note that during the tensile tests the tensile force increased even after the necking indicating a strong hardening mechanism during the tests.

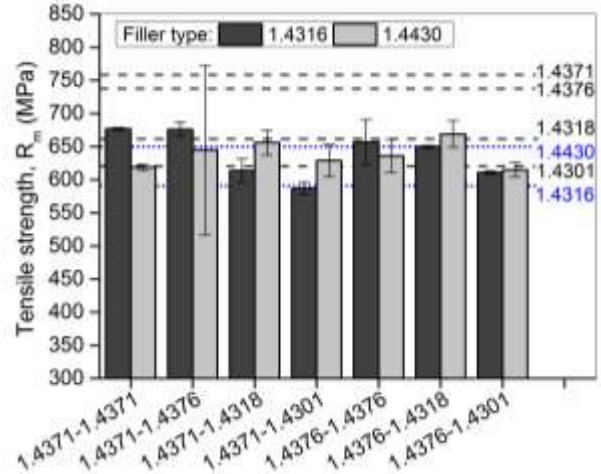

Figure 7. *Ultimate tensile strength of the used base materials (nominal) and the measured values of the welded joints with two types of filler material*

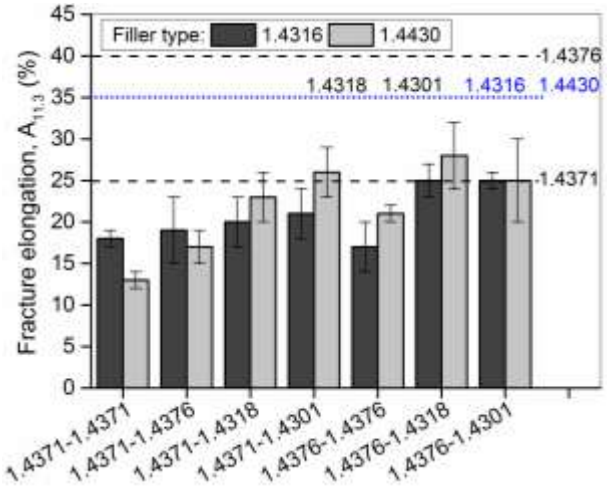

Figure 8. *Fracture elongation values of the base materials (nominal) and the measured values of the welded joints with two types of filler material*

To compare the deformations in the different joint combinations in Fig. 9 the total uniform elongations of the materials (far from necking) until fracture, and the whole elongation of measurement length (including half of the weld material) for both sides corresponding to $A_{5.65}$ is visualized. As excepted the heterogeneous (1.4371-1.4371 and 1.4376-1.4376) specimens had the same elongation values at both sides. If the Cr-Mn 1.4371 joined to 1.4376 as excepted; the 1.4376 side (more deformable see Fig. 8) had more elongations as well with the joint as well the base material welded with both filler types. As for the joints with Cr-Ni ausenitic grades, the 1.4318 and 1.4301 sides always had the greater elongation values with both filler types.

The necking values at fracture were between 43-56 % for all the specimens for both filler types (Tab. 5). Basically, within the scatter range the different joints were in the same range for necking.

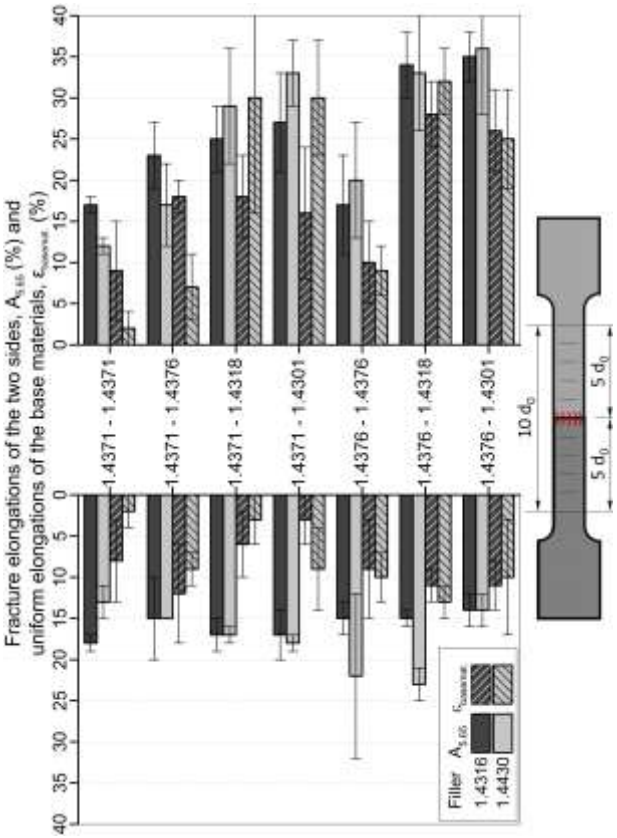

Figure 9. *Fracture elongation values of the two sides of the joints and the uniform elongation values of the base materials in the different joint types*

Table 5. *Necking values and fracture sides of the tensile specimens*

	Sheet grade	Fracture side	Sheet grade	Necking Z (%)
1.4316 filler	**1.4371**	● ► ►	**1.4371**	43±1
	1.4371	◄ ◄ ►	**1.4376**	48±9
	1.4371	◄ ◄ ►	**1.4318**	51±5
	1.4371	◄ ► ►	**1.4301**	49±1
	1.4376	◄ ► ►	**1.4376**	56±6
	1.4376	► ► ►	**1.4318**	47±2
	1.4376	► ► ►	**1.4301**	45±4
1.4430 filler	**1.4371**	◄ ◄ ►	**1.4371**	49±1
	1.4371	◄ ◄ ►	**1.4376**	50±4
	1.4371	◄ ◄ ◄	**1.4318**	50±2
	1.4371	● ► ►	**1.4301**	48±3
	1.4376	◄ ◄ ►	**1.4376**	51±2
	1.4376	◄ ◄ ◄	**1.4318**	45±7
	1.4376	► ► ►	**1.4301**	51±7

Location of the fracture within the WM:
◄ 1st steel grade side,
● weld metal center line,
► 2nd steel grade side.

The fracture of the joint combinations welded with with the 1.4371 Cr-Mn austenitic steel grade occurred mostly on the 1.4371 side with the exception of the 1.4301 grade for both filler types.

Whilst in the joint combinations with the 1.4376 Cr-Mn austenitic steel grade the fracture occurred in opposite steel side, with the exception of 1.4301 grade welded with 1.4430 filler.

Hardness measurements

On the metallographic samples the hardness profiles were measured in ~0.5 mm depth from the top side of the sheets (e.g. Fig. 10). On these hardness profiles the hardness values of HAZ 1-2 and the WM were determined (Tab. 6). The hardness values in HAZ1-2 for one grade is about the same in every joint combinations, for 1.4371 between 200-258 HV0.5, for 1.4376 between 211-245 HV0.5, for 1.4318 between 288-215 HV0.5 and for 1.4301 between; 176-194 HV0.5.

For both filler types, the hardness of the WM (centerline) was higher than the nominal hardness of the filler metal in case of the joint combinations with the high Mn content steel grades(1.4371-1.4371, 1.4371-1.4376 and 1.4376-1.4376), for the other joint combinations the hardness of the WM centerline were lower than the nominal values. For the 1.4318 filler, the WM hardness varied between 185-207 HV0.5, for the 1.4430 filler between 186-200 HV0.5.

It seems that through the dilution the Mn content increases the overall hardness of the joints.

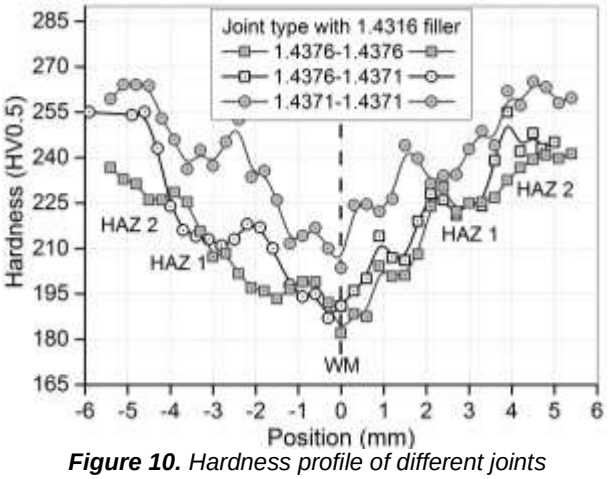

Figure 10. *Hardness profile of different joints welded with 1.4316 filler*

Table 6. *The average hardness values in the different HAZ parts and in the WM*

	Sheet grade	Hardness values (HV0.5) HAZ 2	HAZ 1	WM	HAZ 1	HAZ 2	Sheet grade
1.4316 filler	**1.4371**	257±8	238±6	217±8	238±8	258±7	**1.4371**
	1.4371	252±6	215±3	198±8	221±8	246±7	**1.4376**
	1.4371	240±6	200±3	185±5	188±7	206±3	**1.4318**
	1.4371	246±6	221±5	186±5	177±6	192±6	**1.4301**
	1.4376	229±4	211±5	195±6	223±7	238±4	**1.4376**
	1.4376	245±3	217±4	188±4	189±9	199±5	**1.4318**
	1.4376	245±4	218±6	185±3	177±8	191±5	**1.4301**
1.4430 filler	**1.4371**	245±14	216±4	200±4	219±5	242±6	**1.4371**
	1.4371	244±10	209±8	192±4	234±5	244±3	**1.4376**
	1.4371	251±9	212±5	187±3	202±7	215±8	**1.4318**
	1.4371	258±9	224±8	188±6	184±4	193±4	**1.4301**
	1.4376	237±3	220±3	193±7	218±6	234±3	**1.4376**
	1.4376	242±3	216±7	188±3	198±5	205±3	**1.4318**
	1.4376	245±5	215±8	186±4	176±5	194±3	**1.4301**

For the further comparison of the welded properties of the Mn alloying of austenitic steels further corrosion tests are planned.

4 Conclusions

From the above described investigations the following conclusions can be drawn:

- The 1.4371, 1.4376 (Cr-Mn+N alloyed) austenitic steel grades, the 1.4318 (Cr-Ni+N alloyed) and 1.4301 (Cr-Ni alloyed) austenitic steel grades can be successfully joined in the 2 mm sheet thickness range with 0,27-0,35 kJ·mm^{-1} heat input range, with 1.4316 and 1.4430 filler materials via GTAW.
- Comparing the different steel grades in HAZ 1 the 1.4371 grade had the largest grain coarsening following 1.4318, 1.4376 and 1.4301 in decreasing order. The grain coarsening in HAZ 2 was the largest in the 1.4318 grade, following the 1.4371 steel. The 1.4376 had the initial grain size in HAZ 2 and in 1.4301 steel there was even grain refinement.
- The ultimate tensile strength of the joints varied between; 600-670 MPa and the fracture elongations ($A_{11.3}$) between 13-25 %. The elongation among the different steel grades in the welded joint types was the greatest in the 1.4301 grade following in the 1.4318, 1.4376 and 1.4371 grades.
- The hardness values in the WM and HAZ's increased with the increasing Mn content of the base metal sheets.

5 Acknowledgements

The authors want to thank the Hungarian Welding Society (MAHEG) for financing the participation on the YPIC 2017 conference.

This research was supported by Arcelormittal FCE Hungary Kft. and Outokumpu Distribution Hungary Kft. with the steel materials.

Special thanks to Tamás Törköly from the Dunakeszi Járműjavító Kft. for technical support.

This paper was supported by the János Bolyai Research Scholarship of the Hungarian Academy of Sciences grant number: BO/00294/14 and by The Hungarian Research Fund, NKTH-OTKA PD 120865 (K. Májlinger).

6 Bibliography

[1] Chater J. What prospects for stainless steel in 2016? *Stainl Steel World*. 2016;(January/February):1-5.

[2] Dobránszky J, Varbai B. A króm-mangán ötvözésű ausztenites acélok és hegesztésük. *Hegesztéstechnika*. 2016;27(3):33-38.

[3] BSSA. 200 Series Stainless Steel. *Stainl Steel Ind*. 2006;(August).

[4] Dobránszky J, Sándor T. Új trendek a korrózióálló acélok hegesztésében. *Hegesztéstechnika*. 2008;19(3):8-13.

[5] Charles J, Mithieux J-D, Krautschick J, et al. A new European 200 series standard to substitute 304 austenitics. *Rev Métallurgie*. 2009;106(2):90-98.

[6] Speidel MO. Nitrogen Containing Austenitic Stainless Steels. *Materwiss Werksttech*. 2006;37(10):875-880.

[7] ISSF. “New 200-series” steels: An opportunity or a threat to the image of stainless steel? 2005;(November):1-11.

[8] Charles J. The new 200 series: an alternative answer to Ni surcharges? *Stainl Steel World*. 2007;(May):23-33.

[9] Pauze N, Boillot P, Fanica A, Peultier J. Low Cost Stainless Steels , From Classic 304L/316L To Lean Duplex and 200-Series Materials. In: *Duplex World 2010 Conference*. Beaune, France; 2010.

[10] Charles J, Kosmac A, Kraustschick J, Simon J., Suutala N, Taulavuori T. Austenitic Chromium-Manganese Stainless Steels – A European Approach. *Mater Appl Ser*. 2012;12:1-17.

[11] Pistorius PC, Toit M. Low-Nickel Austenitic Stainless Steels: Metallurgical Constraints. In: *The Twelth International Ferroalloys Congress; Sustainable Future*. ; 2010:911-918.

[12] Mathur NC. Bright future dawning for India's stainless industry. *Stainl Steel World*. 2015;(November):1-4.

[13] Manganese Prices and Manganese Price Charts. http://www.infomine.com/investment/metal-prices/manganese/. Last visited: 16/7/17

[14] Balogh A, Török I, Gáspár M, Juhász D. Present State and Future of Advanced High Strength Steels. 2012;5(1):79-90.

[15] Dobránszky J, Kovács D. Szemlézés a rozsdamentes acélok gyártásának európai kutatásaiból. *BÁNYÁSZATI KOHÁSZATI LAPOK-KOHÁSZAT*. 2016;149(1):6-10.

[16] Kerr J, Paton R. Preliminary Investigations of Low-Nickel Stainless Steels for Structural Applications. In: *Tenth International Ferroalloys Congress*. ; 2004:757-765.

[17] Khobragade NN, Khan MI, Patil AP. Corrosion behaviour of chrome-manganese austenitic stainless steels and AISI 304 stainless steel in chloride environment. *Trans Indian Inst Met*. 2014;67(2):263-273.

[18] Schwind M, Falkenberg F, Johansson E, Larsson J. Properties of various low-nickel stainless steels in comparison to AISI 304. *Stainl Steel World*. 2008;(March):66-77.

[19] Coetzee M, Pistorius PGH. The welding of experimental low-nickel Cr- Mn- N stainless steels containing copper. *J South Sfrican Inst Min Metall*. 1996;(May/June):99-108.

[20] Espy RH. Weldability of Nitrogen-Strengthened Stainless Steels. *Weld J*. 1982;(May):149-156.

[21] Bonnefois B, Peultier J, Serriere M, Hauser J-M, Chauveau E. Acier inoxydable duplex. 2012:1-25.

[22] Brooks JA. Weldability of High N , High Mn Austenitic Stainless Steel. *Weld Res Suppl*. 1975;(June):189-195.

[23] Haraszti F, Kovacs T. Plastic deformation effect of the corrosion resistance in case of austenitic stainless steel. In: *IOP Conf. Series: Materials Science and Engineering*. Vol 175. ; 2017.

[24] Urade VP, Ambade SP. An Overview of Welded Low Nickel Chrome-Manganese Austenitic and Ferritic Stainless Steel. *J Mater Sci Eng*. 2016;5(2):1-6.

[25] Kartik B, Veerababu R, Sundararaman M, Satyanarayana DVV. Effect of high temperature ageing on microstructure and mechanical properties of a nickel-free high nitrogen austenitic stainless steel. *Mater Sci Eng A*. 2015;642:288-296.

[26] Vashishtha H, Taiwade RV, Khatirkar RK, Ingle AV, Dayal RK. Welding Behaviour of Low Nickel Chrome-Manganese Stainless Steel. *ISIJ Int*. 2014;54(6):1361-1367.

[27] Bharwal S, Vyas C. Weldability Issue of AISI 202 SS (Stainless Steel) Grade with GTAW Process Compared to AISI 304 SS Grade. *Int J Adv Mech Eng*. 2014;4(6):695-700.

[28] Chuaiphan W, Srijaroenpramong L. Effect of welding speed on microstructures, mechanical properties and corrosion behavior of GTA-welded AISI 201 stainless steel sheets. *J Mater Process Technol*. 2014;214(2):402-408.

[29] Vigneshvar VS, Sudhakaran R. A Review on Performance Improvement in the Weldment Regions of Chromium Manganese Stainless Steels (AISI 202 SS). *Int J Res Appl Sci Eng Technol*. 2014;2(11):416-419.

[30] Dobránszky J, Sándor T, Nagy-Hinst A, Eichhardt AG, Gyura L. Weld Pool Characteristics of the ATIG-Welded Joints. In: *Duplex 2007: International Conference and Expo*. Grado, Italy; 2007.

[31] Choubey A, Jatti VS. Influence of heat input on mechanical properties and microstructure of austenitic 202 grade stainless steel weldments. *WSEAS Trans Appl Theor Mech*. 2014;9(1):222-228.

[32] Vashishtha H, Taiwade RV, Khatirkar RK, Dhoble AS. Effect of austenitic fillers on microstructural and mechanical properties of ultra-low nickel austenitic stainless steel. *Sci Technol Weld Join*. 2016;21(4):331-337.

[33] Collur MM, Debroy T. Emission spectroscopy of plasma during laser welding of AISI 201 stainless steel. *Metall Mater Trans B*. 1989;20(2):277-286.

[34] Chandra-Ambhorn S, Chauiphan W, Sukwattana NC, Pudkhunthod N, Komkham S. Plasma Arc Welding between AISI 304 and AISI 201 Stainless Steels Using a Technique of Mixing Nitrogen in Shielding Gas. *Adv Mater Res*. 2012;538-541:1464-1468.

[35] Ikram A, Khan MI, Moeed KM. Comparative Study of Spot Welding Process Parameters on Microstructure and Mechanical Properties of ASS 304 and ASS 202 Steel. *Int J Mech Ind Technol*. 2015;3(1):35-39.